Chem. Chem. Technol., 2025,
Vol. 19, No. 3, pp. 455–462

Chemistry

OXIDATIVE CO_2 DEHYDROGENATION OF n-BUTANE ON MICROSPHERICAL ZEOLITE-CONTAINING COMPOSITES BASED ON UKRAINIAN KAOLIN

Oleksandra Pertko[1,✉], Yuliya Voloshyna[1], Lyubov Patrylak[1, 2], Angela Yakovenko[1]

https://doi.org/10.23939/chcht19.03.455

Abstract. In the present study, zeolite-containing microspherical composites based on Ukrainian kaolin were synthesized and modified with ammonium, lanthanum, and zirconium compounds. The modified composites were dealuminated by thermal steaming. The obtained materials were characterized by various physical and chemical methods and tested in the reaction of oxidative dehydrogenation of *n*-butane with the participation of CO_2. The influence of several factors on the characteristics of the synthesized samples and related changes in their activity and selectivity were analyzed. The results of the work showed the possibility of using such composites as catalysts for this reaction.

Keywords: kaolin microsphere, FAU zeolite, composite catalyst, transition metal, oxidative dehydrogenation, *n*-butane.

1. Introduction

The main process aimed at deepening oil refining is catalytic cracking. As a result, in addition to the gasoline fraction, a significant amount of gas rich in unsaturated hydrocarbons (UHs) is produced. Light UHs, due to their high reactivity compared to their saturated counterparts, are indispensable chemical building blocks in the petrochemical industry and can be used to produce valuable petroleum products. In particular, 1,3-butadiene (1,3-BD) is an important raw material for petrochemical production and a material for various industries. Today, it is produced mainly by cryogenic distillation of the C_4 fraction of crude oil cracking.[1,2] However, ever-growing demand for butadiene has stimulated the search for alternative production technologies.

For example, approaches are developing for 1,3-BD production by ethanol conversion[3–7] or through dehydrogenation of butane, both non-oxidative[8,9] and oxidative.[10–12] This is facilitated by the availability of large quantities of alkane raw materials from shale gas and other sources.[13] Dehydrogenation of alkanes is a promising reaction for the production of olefins, and the development of new catalysts for this reaction is now of current importance.[14] The inclusion of an oxidizing agent has a positive effect on the activity of catalysts and their resistance to coking. Thanks to the oxidant, less energy is consumed, and unwanted cracking reactions are suppressed. O_2 is commonly used as an oxidant in oxidative dehydrogenation reactions of hydrocarbons,[15] but in the case of butane, O_2 contributes to a decrease in the selectivity of catalysts for butenes/butadiene due to their high reactivity and deep oxidation to CO_2 and H_2O.[16] The use of sulfur-containing compounds,[17,18] N_2O[18–20] and halogens[18] as oxidants instead of or together with oxygen or air has been studied. However, the vast majority of studies focus on CO_2,[18,20,21] because the mild nature of the oxidant prevents excessive oxidation of hydrocarbons in oxidative dehydrogenation with the participation of CO_2 (CO_2-OD). The requirements for CO_2-OD catalysts are efficient activation of CO_2 and selective activation of C–H bonds of hydrocarbons with inhibition of C–C bond activation/breaking while maintaining high catalytic activity.[22]

FAU (Y),[23] BEA (Beta),[24] and MFI (ZSM-5)[25] zeolites modified by dealumination[24] and impregnated with Zn,[26] Cr, and/or V[23–25] compounds are considered as the basis of zeolite catalysts for the dehydrogenation of light alkanes. Carriers with moderate[23] or low[24] acidity, achieved by dealumination, are preferred, apparently because they inhibit undesirable side reactions of cracking. The disadvantage of existing zeolite catalysts is their low activity. The preparation of an active catalyst with high selectivity for butenes and 1,3-BD, which would provide high yields of olefins, remains one of the most important problems in the dehydrogenation of n-butane. Among zeolites, natural materials are of great interest due to their availability and low cost. Modified natural zeolites are used

[1] V.P. Kukhar Institute of Bioorganic Chemistry and Petrochemistry of the NAS of Ukraine, 1 Akademika Kukharia St., Kyiv 02094, Ukraine
[2] National Technical University of Ukraine "Igor Sikorsky Kyiv Polytechnic Institute", 37 Beresteiskyi Ave., Kyiv 03056, Ukraine
✉ *o.pertko@gmail.com*
© Pertko O., Voloshyna Yu., Patrylak L., Yakovenko A., 2025

as catalysts for many acid-base[27,28] and redox[29–31] reactions. However, few studies have been devoted to the oxidative dehydrogenation of light alkanes in the presence of natural zeolites.

One of the ways to increase the efficiency of catalysts for CO_2-OD of light alkanes can be the use of zeolite-containing microspheres, since the use of zeolite in the form of a thin surface layer will reduce the role of micropores as diffusion barriers, reducing the diffusion path of reaction products in the space where active sites are concentrated. This will increase the selectivity for target dehydrogenation products, restraining the course of secondary reactions involving them, such as cracking, oligomerization, aromatization, etc., as well as reduce coke formation. The latter is an important factor in the efficiency of catalysts for this reaction, considering the high concentration of UHs in the reaction space.

Taking into account the relevance of finding new active and selective catalysts for the production of light UHs, the aim of this work was to determine the catalytic activity in the reaction of CO_2-OD of *n*-butane of microspherical composites synthesized on the basis of Ukrainian kaolin, the zeolite phase of which was modified by the introduction of La and Zr for bringing in Lewis acidity, and dealuminated by steaming.

2. Experimental

2.1. Materials

Kaolin from the Prosyanivske deposit (Ukraine) was used as a raw material for the synthesis of zeolite-containing microspheres according to a known method.[32] To begin, kaolin microspheres were calcined at 700 °C to obtain metakaolin microspheres (MSmk) and at 1000 °C to obtain microspheres of aluminosilicate spinel mixed with active SiO_2. In the next step, both types of microspheres were mixed and subjected to hydrothermal treatment in an aqueous NaOH solution to produce a zeolite-containing microspherical composite (about 30 wt% of Y-type zeolite). After that, the composite was converted to the protonic form by 4-fold ion exchange with an aqueous solution of NH_4NO_3 (3 mol/L) followed by calcination at 550 °C (HMS sample). Lanthanum and zirconium were introduced into the composite from aqueous solutions of $La(NO_3)_3$ (LaMS sample, 3.5 wt% of La) and $ZrOCl_2$ (ZrMS sample, 4.5 wt% of Zr), respectively. Thermal steam dealumination of the samples was carried out at 800 °C, 2 hours (deLaMS and deZrMS samples). The zeolite content in the dealuminated samples was 12 wt% and 15 wt% for deLaMS and deZrMS, respectively.

2.2. Methods

Isotherms of low-temperature (–196 °C) nitrogen adsorption/desorption were measured on a NOVA 1200e automatic sorptometer (Quantachrome Instruments) after evacuating the samples in situ at a temperature of 250 °C for 3 h. NovaWin software was used to calculate the parameters of a porous structure of the composites. The specific surface area (S^{BET}) was calculated using the multipoint BET method; the specific surface area excluding micropores (S^t) and the volume of micropores (V_{micro}) – by the t-method, using the de Boer equation; the specific surface area of micropores (S_{micro}) – as $S^{BET} – S^t$; the total pore volume (V) – as the volume of adsorbed nitrogen at p/p_0 ~0.99. The volume of mesopores (V_{meso}) was calculated as $V – V_{micro}$, considering the proportion of macropores to be insignificant. Pore size distribution was determined using density functional theory (DFT).

FTIR spectra of the composites in the field of framework vibrations (400–1400 cm^{-1}) were recorded on the IRAffiniti-1s Fourier spectrometer (Shimadzu) with a single-reflection ATR accessory Specac Quest GS 10801-B. A sample was applied to the surface of the diamond prism of the ATR accessory, and the spectrum relative to air was recorded.

The acid characteristics of the composites were studied by the method of thermally programmed desorption (TPD) of probe molecules (NH_3) from their surface using an automatic system AMI-300Lite (Altamira Instruments). The samples were activated in a He flow at 500 °C, after which they were cooled to a temperature of 200 °C, and ammonia adsorption was carried out for 30 min. Physically adsorbed probe molecules were removed by purging in a He flow. Desorption of NH_3 from the surface of the samples was carried out by linearly increasing the temperature to 500 °C and holding at this temperature for 30 min.

The catalytic tests were carried out on a setup based on a CrystalLux 4000M chromatograph with a quartz reactor. The chromatographic unit is equipped with two types of detectors: a PID for analyzing hydrocarbon components and a TCD for analyzing carbon oxides. Hydrocarbon components were separated on an Agilent J&W GC-ALUMINA capillary column (phase – Al_2O_3, 50 m, inner diameter 0.535 mm), and carbon oxides on a packed column filled with SCN activated carbon (50 m, inner diameter 3 mm). Catalyst samples (150 mg) were activated at 450 °C for 30 min in an Ar flow. The reaction was carried out in the temperature range of 450–650 °C with a step of 50 °C. Reaction conditions: $WHSV_{C4H10}$ = 3.6 h^{-1}, volume ratio of the components of the reaction mixture and carrier gas $C_4H_{10}/CO_2/Ar$ = 1/2/17, flow rate 70 ml/min, reaction duration 10 min until sampling for analysis. Analysis conditions: injector – 120 °C; thermostat of the columns – 100 °C (for the capillary column,

programmed heating was set to 190 °C at a rate of 10 °C/min from 15 minutes of analysis with a 6 minutes holding time at the final temperature); inlet pressure to the capillary column – 0.15 atm, split ratio – 1:60; flow through the packed column – 30 ml/min; PID temperature – 120 °C (flows through the detector: H_2 – 30 mL/min, air – 350 mL/min, Ar – 30 mL/min); TCD temperature – 120 °C (flow through the shoulders – 30 mL/min); analysis time – 30 min.

Based on the chromatographic analysis, the conversion of butane (X (mol% C1)), the selectivity for reaction products (S_j (mol/100 mol of converted butane)), and their yield (Y_j (mol% C1)) were calculated by formulas (1)–(3):

$$X = \frac{\sum C_j}{\sum C_j + C} \times 100\%, \quad (1)$$

$$S_j = \frac{4}{n_j} \times \frac{C_j}{\sum C_j} \times 100, \quad (2)$$

$$Y_j = \frac{n_j}{4} \times \frac{X \times S_j}{100}, \quad (3)$$

where C_j is the concentration of C-atoms of the identified carbon-containing j-product in the reaction products (vol%); C is the concentration of C-atoms of unconverted butane in the reaction products (vol%); n_j is a number of C-atoms in the identified carbon-containing j-product.

3. Results and Discussion

3.1. Physical-chemical properties of the composites

In Fig. 1, N_2 adsorption/desorption isotherms and pore size distribution for metakaolin microspheres and zeolite-containing composites on their basis are shown. Fig. 2 demonstrates a comparative view of the porous characteristics of the samples.

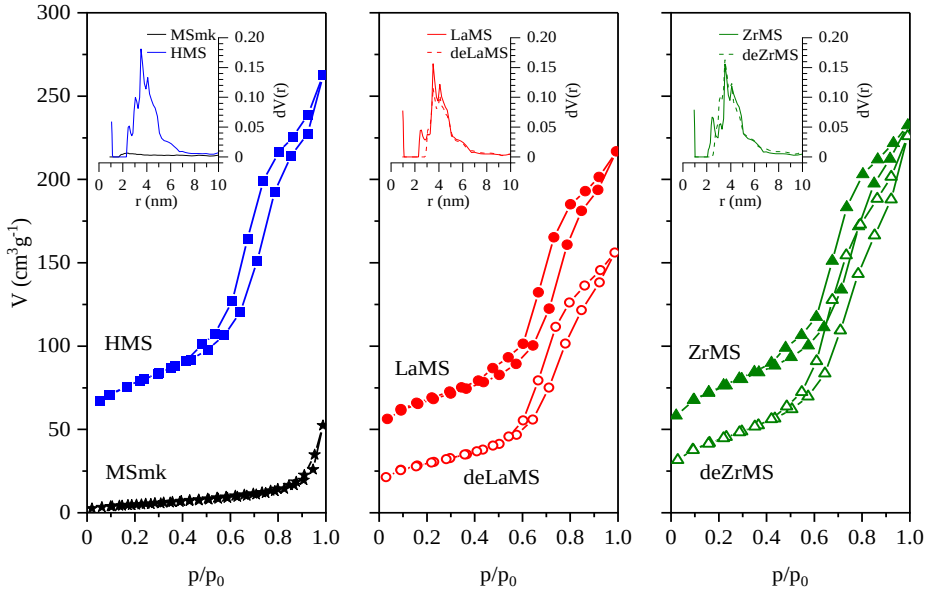

Fig. 1. N_2 adsorption/desorption isotherms and DFT pore size distribution for metakaolin microspheres and zeolite-containing composites on their basis

According to the adsorption data, metakaolin microspheres are characterized by low porosity in general and do not have any microporosity. As a result of the synthesis, microspheres acquire both micro- and mesoporosity. The character of the pore size distribution for all zeolite-containing composites is similar and remains the same after dealumination. The composites contain mesopores with a diameter of 4–13 nm. Most of them are characterized by a size of about 8 nm. The number of pores decreases slightly after the introduction of lanthanum and zirconium, especially in the case of the La-containing sample. Micropores in the initial, non-dealuminated samples make up about 15% of the total porosity.

After dealumination, the specific surface area decreases due to a lessening of microporosity. The proportion of micropores drops by an order of magnitude. At the same time, the number of mesopores remains almost the same, which is most pronounced for the Zr-containing sample.

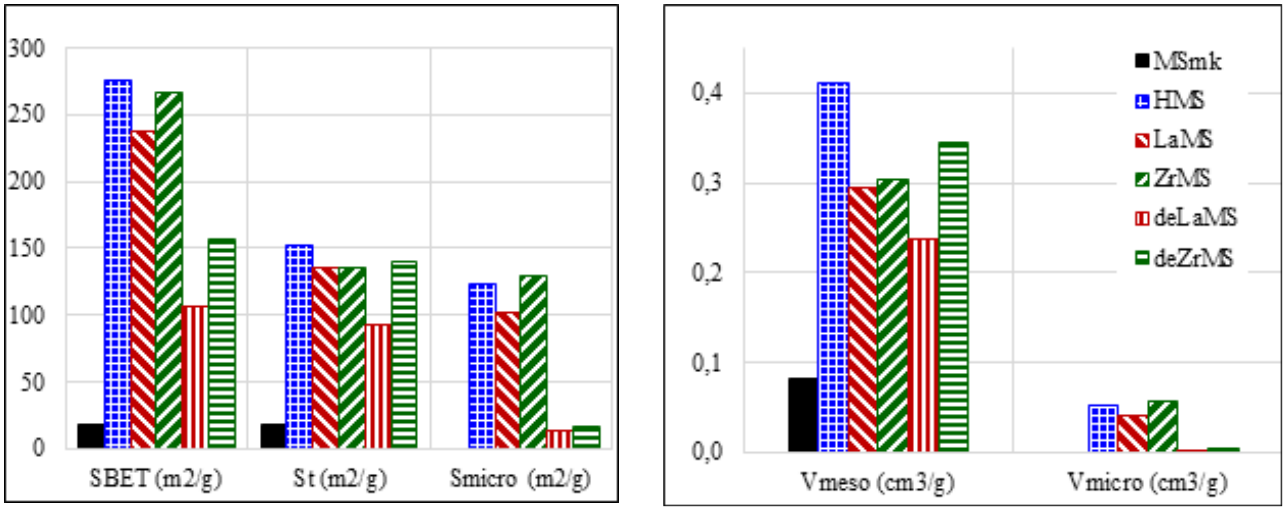

Fig. 2. Porosity characteristics of metakaolin microspheres and studied zeolite-containing composites

Dealumination of the samples is confirmed by the analysis of their FTIR spectra in the region of framework vibrations, in particular, by the high-frequency shift of the absorption band corresponding to the antisymmetric stretching vibrations of T–O bonds of framework tetrahedra, from 1020 cm^{-1} to 1060 cm^{-1} (Fig. 3A).

The total content of acid sites in the samples was estimated by TPD of ammonia. The analysis of the ammonia TPD profiles (Fig. 3B) showed that the initial samples (curves 1–3) contain acid sites characterized by maxima in the range of 250–400 °C, that is, they are sites of medium strength with a slight predominance of weaker ones. In the LaMS and deLaMS samples, the content of weaker acid sites is the lowest in their group (curves 2, 2'), while stronger sites slightly prevail in the LaMS sample before dealumination. After dealumination, the samples (curves 2', 3') lose a significant part of the sites; the strength of the sites does not undergo noticeable changes. This correlates with the loss of microporosity in the dealuminated samples. Thus, the acid characteristics of the studied composites are similar and remain so after dealumination, regardless of the metal introduced.

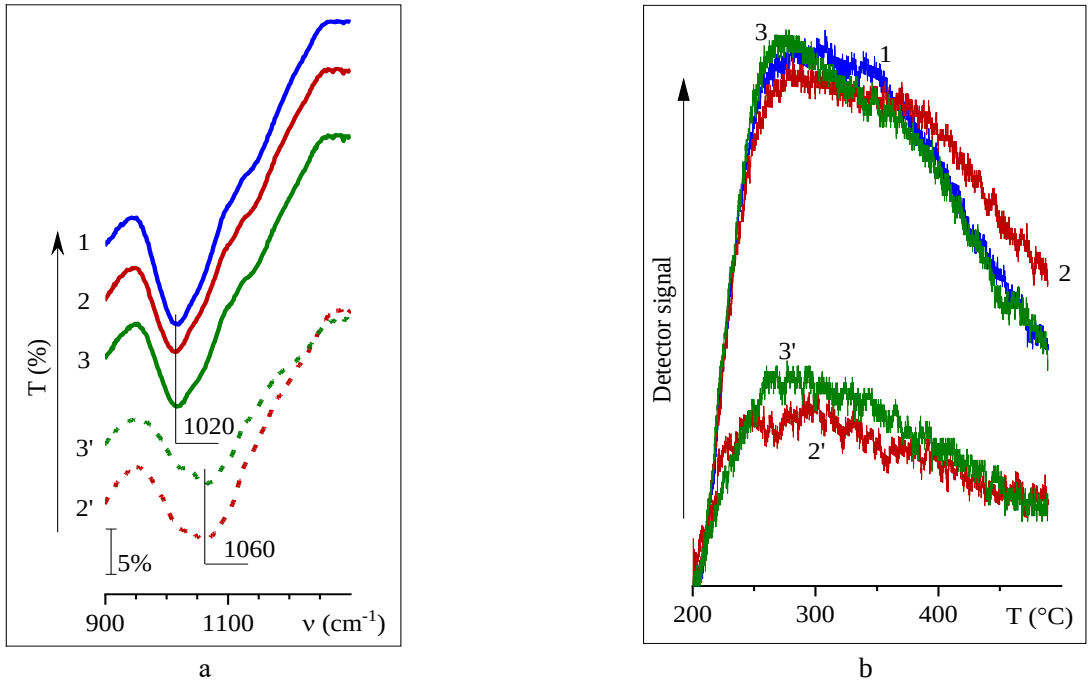

Fig. 3. (**A**) Fragments of FTIR spectra and (**B**) ammonia TPD profiles of the (1–3) initial and (2', 3') dealuminated zeolite-containing composites (1) HMS, (2, 2') LaMS, and (3, 3') ZrMS

3.2. Catalytic properties of the composites in the reaction of CO_2-OD of butane

The reaction was carried out both in the presence and without a catalyst. In the blank experiment without a catalyst, the conversion does not depend on the presence of CO_2 in the system, as does the selectivity for butane dehydrogenation products (C_4-UHs) at significant conversion values (Fig. 4). In both cases, the conversion occurs mainly in the direction of formation of cracking products. Obviously, in the absence of a catalyst, thermal cracking occurs. In the presence of a catalyst (HMS), the presence of CO_2 in the system significantly affects the character of the reaction: the degree of butane conversion and selectivity for C_4-UHs increase. Although CO_2 is a thermodynamically stable molecule, there are several ways to activate it on catalytically active surfaces.[33] Comparison of the blank experiments with the experiments in the presence of a catalyst confirms both the catalytic nature of dehydrogenation on the studied composites and the participation of CO_2 in this reaction. As a result, target products (butenes, 1,3-BD, and C_2–C_3 UHs) and by-products (C_1–C_3 alkanes) were formed (Fig. 5).

The HMS sample in the protonic form is the most active: butane conversion on it begins to increase from 500 °C (Fig. 4A). On La- and Zr-containing composites, the activation of transformations is shifted towards higher temperatures by 50–100 °C (initial and dealuminated samples, respectively) compared to HMS. At the beginning of the reaction, the main products are dehydrogenation products – C_4-UHs (Fig. 4B). Selectivity for them decreases with increasing temperature due to intensification of cracking to C_1–C_3 hydrocarbons. As a result, the yield of the latter, in particular C_2–C_3 UHs, becomes predominant (Fig. 5). Obviously, the introduction of metals into the composite inhibits the process of cracking of C_4 hydrocarbons, since the yield of butenes in LaMS and ZrMS samples, unlike HMS, regularly increases with the degree of conversion, as well as the yield of the most valuable 1,3-BD.

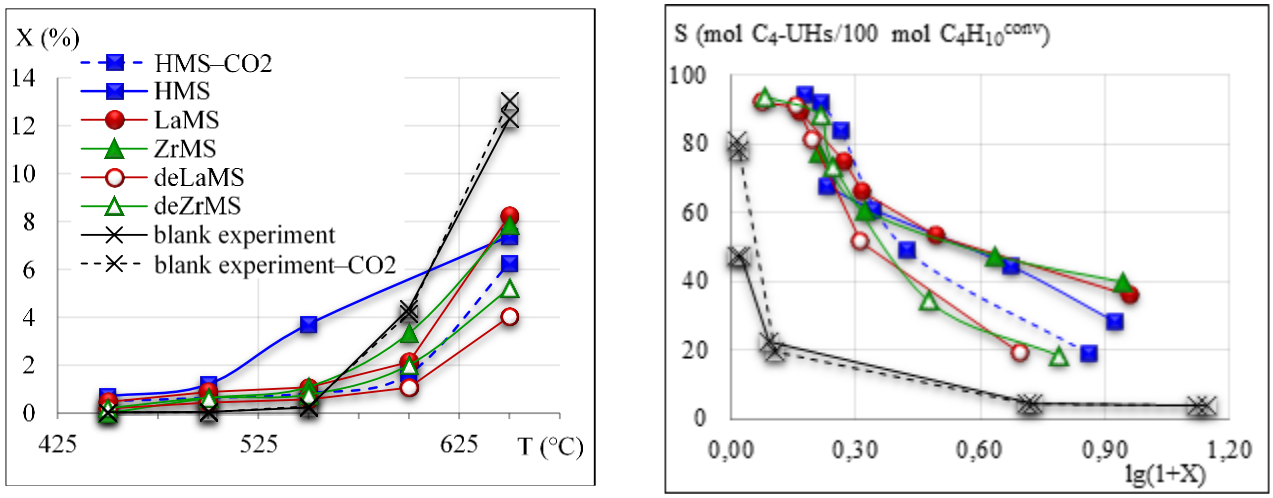

Fig. 4. (**A**) Butane conversion and (**B**) selectivity for C_4-UHs obtained on samples of microspherical composites of different composition and without a catalyst. Experiments that did not use CO_2 are marked "–CO_2"

The La- and Zr-containing composites show similar catalytic behavior (Fig. 4, 5). At the same time, Zr seems to inhibit the cracking of C_4 hydrocarbons somewhat more effectively, while the La-containing sample is somewhat more effective in dehydrogenating butenes to 1,3-BD (Fig. 5).

The selectivity of deLaMS and deZrMS samples for target products increases, but at very low conversion degrees, and this concerns only the most valuable isomer, 1,3-BD. However, this is quickly lost as the conversion degree increases. The reverse side of dealumination is both the partial loss of the active surface due to the thermal steam treatment procedure and the decrease in the basicity of the zeolite framework caused by its depletion in aluminum. This results in less efficient adsorption and activation of CO_2 on the dealuminated composite, which is supported by the similar character of the dependences obtained for the dealuminated samples, on the one hand, and the HMS sample tested in the absence of CO_2, on the other hand (Fig. 5). The same conclusion was reached by Alvarez and co-workers[33] based on calculations of the characteristic OCO angle and CO bond length of the CO_2

molecule in various adsorbed forms. They stated that the formation of a bent and reactive CO_2 on the surface of oxides is promoted by more basic oxides. The effect of dealumination, similar to that caused by the absence of CO_2, has the consequence of a sharp decrease in the selectivity for dehydrogenation products. As a result, in the case of dealuminated samples, a decrease in the yield of C_4-UHs is observed against the background of an increase in the yield of cracking products at the same conversion rates, since the latter are achieved at a higher temperature.

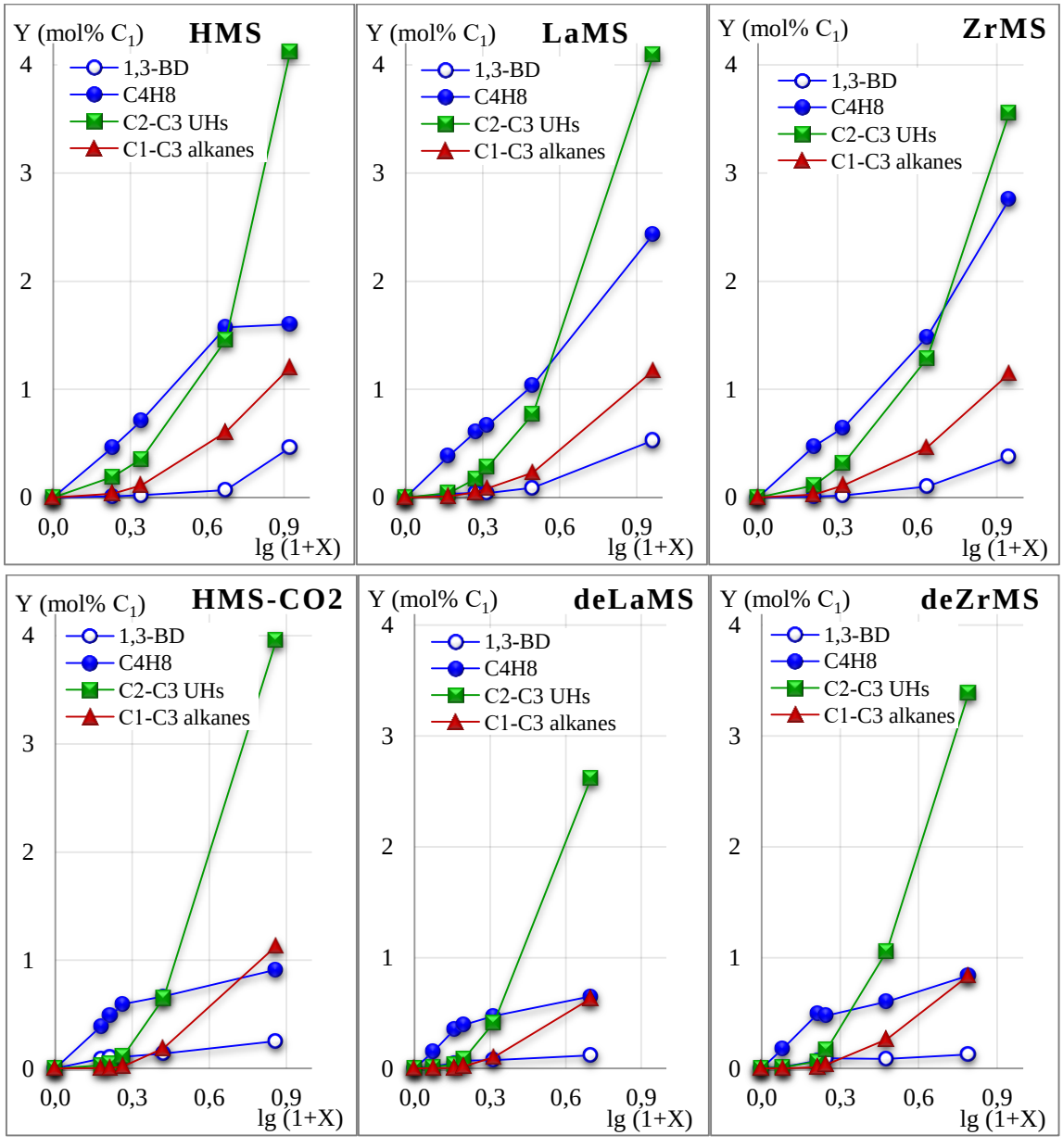

Fig. 5. Yields of butane conversion products on samples of microspherical composites of different composition

4. Conclusions

In the present study, zeolite-containing microspherical composites based on Ukrainian kaolin were synthesized and modified with ammonium, lanthanum, and zirconium compounds. The modified composites were subjected to thermal steam treatment for dealumination. The physicochemical properties of the obtained materials were characterized using low-temperature nitrogen adsorption/desorption, FTIR spectroscopy, and thermally programmed ammonia desorption.

Samples of the microspherical composites of different compositions were tested in the reaction of oxidative dehydrogenation of butane with the participation

of CO_2, and their activity in this reaction was revealed. It was found that the introduction of La and Zr inhibits the cracking reaction of C_4 hydrocarbons, which leads to an increase in the selectivity of the catalysts for the target C_4-UHs. No distinct differences were observed in the course of the reaction on La- and Zr-containing samples. It was shown that dealumination reduces the conversion of reagents, which is explained by the decrease in the number of acid sites, degradation of the active surface of the samples during steaming, and the decrease in the basicity of their zeolite framework.

Therefore, the results of the work show the possibility of using zeolite-containing microspherical composites modified with La or Zr as catalysts for the reaction of CO_2-OD of butane to C_4-UHs. Increasing the selectivity of the studied composite catalysts for 1,3-BD requires an increase in their oxidation potential, for example, by introducing oxides of a high degree of oxidation. Further studies are needed to classify acid sites by type and strength, as well as to determine the nature of carriers of Lewis acid sites in such composites and the role of these sites in the reaction. Given the negative effect of dealumination on the activity and selectivity of the samples under study, the use of this procedure in the preparation of catalysts seems inappropriate.

Acknowledgements

This work was supported by the National Research Foundation of Ukraine (Project name: Design of nanocomposite metal-oxide catalysts for the compatible oxidative conversion of C1-4-alkanes and carbon dioxide with the production of hydrogen/syngas, valuable organic compounds; Registered project number: 2021.01/0017).

The authors acknowledge the assistance of Candidate of Chemical Sciences O.V. Larina and PhD O.V. Zikrata (L.V. Pisarzhevskii Institute of Physical Chemistry of the National Academy of Sciences of Ukraine) in obtaining the ammonia TPD profiles. The authors also are grateful to the European Chemistry School for Ukrainian (https://ecpsfu.org) for providing an overview of current trends in European chemical science.

References

[1] Ren, T.; Patel, M.; Blok, K. Olefins from Conventional and Heavy Feedstocks: Energy Use in Steam Cracking and Alternative Processes. *Energy* **2006**, *31*, 425–451. https://doi.org/10.1016/j.energy.2005.04.001

[2] Bender, M. An Overview of Industrial Processes for the Production of Olefins – C_4 Hydrocarbons. *ChemBioEng Rev*. **2014**, *1*, 136–147. https://doi.org/10.1002/cben.201400016

[3] Cespi, D.; Passarini, F.; Vassura, I.; Cavani, F. Butadiene from Biomass, a Life Cycle Perspective to Address Sustainability in the Chemical Industry. *Green Chem*. **2016**, *18*, 1625–1638. https://doi.org/10.1039/C5GC02148K

[4] Kyriienko, P. I.; Larina, O. V.; Soloviev, S. O.; Orlyk, S. M.; Calers, C.; Dzwigaj, S. Ethanol Conversion into 1,3-Butadiene by the Lebedev Method over MTaSiBEA Zeolites (M = Ag, Cu, Zn). *ACS Sustainable Chem. Eng*. **2017**, *5*, 2075–2083. https://doi.org/10.1021/acssuschemeng.6b01728

[5] Larina, O. V.; Kurmach, M. M.; Kyriienko, P. I.; Alekseenko, L. M.; Shvets, O. V.; Soloviev, S. O. Influence of Acid–Base Characteristics of Hierarchical Cu/Zr-MTW Zeolites on Their Catalytic Properties in 1,3-Butadiene Production from Ethanol–Water Mixtures. *Theor. Exp. Chem*. **2021**, *57*, 343–350. https://doi.org/10.1007/s11237-021-09703-4

[6] Kyriienko, P. I.; Larina, O. V.; Balakin, D. Yu.; Soloviev, S. O.; Orlyk, S. M. Influence of Copper and Silver on Catalytic Performance of $MgO–SiO_2$ System for 1,3-Butadiene Production from Aqueous Ethanol. *Catal. Lett*. **2022**, *152*, 921–930. https://doi.org/10.1007/s10562-021-03704-7

[7] Larina, O. V.; Zikrata, O. V.; Alekseenko, L. M.; Soloviev, S. O.; Orlyk, S. M. The Effect of Modification of Zn–Mg(Zr)Si Oxide Catalysts with Rare-Earth Elements (Y, La, Ce) in the Ethanol-to-1,3-Butadiene Process. *Appl. Nanosci*. **2023**, *13*, 7101–7114. https://doi.org/10.1007/s13204-023-02876-5

[8] Sattler, J. J. H. B.; Ruiz-Martinez, J.; Santillan-Jimenez, E.; Weckhuysen, B. M. Catalytic Dehydrogenation of Light Alkanes on Metals and Metal Oxides. *Chem. Rev*. **2014**, *114*, 10613–10653. https://doi.org/10.1021/cr5002436

[9] Camacho-Bunquin, J.; Ferrandon, M. S.; Sohn, H.; Kropf, A. J.; Yang, C.; Wen, J.; Hackler, R. A.; Liu, C.; Celik, G.; Marshall, C. L.; Stair, P. C.; Delferro, M. Atomically Precise Strategy to a PtZn Alloy Nanocluster Catalyst for the Deep Dehydrogenation of *n*-Butane to 1,3-Butadiene. *ACS Catal*. **2018**, *8*, 10058–10063. https://doi.org/10.1021/acscatal.8b02794

[10] Zhang, J.; Liu, X.; Blume, R.; Zhang, A.; Schlögl, R.; Su, D. S. Surface-Modified Carbon Nanotubes Catalyze Oxidative Dehydrogenation of *n*-Butane. *Science* **2008**, *322*, 73–77. https://doi.org/10.1126/science.1161916

[11] Coperet, C. C−H Bond Activation and Organometallic Intermediates on Isolated Metal Centers on Oxide Surfaces. *Chem. Rev*. **2010**, *110*, 656–680. https://doi.org/10.1021/cr900122p

[12] Tanimu, G.; Aitani, A. M.; Asaoka, S.; Alasiri, H. Oxidative Dehydrogenation of N-Butane to Butadiene Catalyzed by New Mesoporous Mixed Oxides NiO-(Beta-Bi_2O_3)-Bi_2SiO_5/SBA-15 System. *Mol. Catal*. **2020**, *488*, 110893. https://doi.org/10.1016/j.mcat.2020.110893

[13] BP. Statistical Review of World Energy 2021. BP p.l.c., 2021. https://www.bp.com/content/dam/bp/business-sites/en/global/corporate/pdfs/energy-economics/statistical-review/bp-stats-review-2021-full-report.pdf (accessed 2024-11-04).

[14] Redkina, A.; Konovalova, N.; Kravchenko, N.; Strelko, V. Influence of the Porous Structure of V_2O_5-ZrO_2-SiO_2 Catalyst on Reaction of Propane Dehydrogenation. *Chem. Chem. Technol*. **2022**, *16*, 259–266. https://doi.org/10.23939/chcht16.02.259

[15] Fedevych, O. Study on Heterogeneous Catalytic Oxidative Dehydrogenation of Isopropylbenzene to α-Methylstyrene. *Chem. Chem. Technol*. **2022**, *16*, 507–514. https://doi.org/10.23939/chcht16.04.507

[16] Murgia, V.; Torres, E.; Gottifredi, J.; Sham, E. Sol–Gel Synthesis of $V_2O_5–SiO_2$ Catalyst in the Oxidative Dehydrogenation of *n*-Butane. *Appl. Catal. A: Gen*. **2006**, *312*, 134–143. https://doi.org/10.1016/j.apcata.2006.06.042

[17] Gaspar, N. J.; Pasternak, I. S. H2S Promoted Oxidative Dehydrogenation of Ethane. *Can. J. Chem. Eng*. **1971**, *49*, 248–251. https://doi.org/10.1002/cjce.5450490213
[18] Jiang, X.; Sharma, L.; Fung, V.; Park, S. J.; Jones, C. W.; Sumpter, B. G.; Baltrusaitis, J.; Wu, Z. Oxidative Dehydrogenation of Propane to Propylene with Soft Oxidants via Heterogeneous Catalysis. *ACS Catal*. **2021**, *11*, 2182–2234. https://doi.org/10.1021/acscatal.0c03999
[19] Pérez-Ramírez, J.; Gallardo-Llamas, A. Impact of the Preparation Method and Iron Impurities in Fe-ZSM-5 Zeolites for Propylene Production via Oxidative Dehydrogenation of Propane with N_2O. *Appl. Catal. A: Gen*. **2005**, *279*, 117–123. https://doi.org/10.1016/j.apcata.2004.10.020
[20] Dasireddy, V. D. B. C.; Huš, M.; Likozar, B. Effect of O_2, CO_2 and N_2O on Ni–Mo/Al_2O_3 Catalyst Oxygen Mobility in *n*-Butane Activation and Conversion to 1,3-Butadiene. *Catal. Sci. Technol*. **2017**, *7*, 3291–3302. https://doi.org/10.1039/C7CY01033H
[21] Gambo, Y.; Adamu, S.; Tanimu, G.; Abdullahi, I. M.; Lucky, R. A.; Ba-Shammakh, M. S.; Hossain, Mohammad. M. CO_2-Mediated Oxidative Dehydrogenation of Light Alkanes to Olefins: Advances and Perspectives in Catalyst Design and Process Improvement. *Appl. Catal. A: Gen*. **2021**, *623*, 118273. https://doi.org/10.1016/j.apcata.2021.118273
[22] Xie, Z.; Tian, D.; Xie, M.; Yang, S.-Z.; Xu, Y.; Rui, N.; Lee, J. H.; Senanayake, S. D.; Li, K.; Wang, H.; *et al*. Interfacial Active Sites for CO_2 Assisted Selective Cleavage of C–C/C–H Bonds in Ethane. *Chem* **2020**, *6*, 2703–2716. https://doi.org/10.1016/j.chempr.2020.07.011
[23] Volpe, M.; Tonetto, G.; De Lasa, H. Butane Dehydrogenation on Vanadium Supported Catalysts under Oxygen Free Atmosphere. *Appl. Catal. A: Gen*. **2004**, *272*, 69–78. https://doi.org/10.1016/j.apcata.2004.05.017
[24] Michorczyk, P.; Zeńczak-Tomera, K.; Michorczyk, B.; Węgrzyniak, A.; Basta, M.; Millot, Y.; Valentin, L.; Dzwigaj, S. Effect of Dealumination on the Catalytic Performance of Cr-Containing Beta Zeolite in Carbon Dioxide Assisted Propane Dehydrogenation. *J. CO2 Util*. **2020**, *36*, 54–63. https://doi.org/10.1016/j.jcou.2019.09.018
[25] Ajayi, B. P.; Rabindran Jermy, B.; Abussaud, B. A.; Al-Khattaf, S. Oxidative Dehydrogenation of *n*-Butane over Bimetallic Mesoporous and Microporous Zeolites with CO_2 as Mild Oxidant. *J. Porous Mater*. **2013**, *20*, 1257–1270. https://doi.org/10.1007/s10934-013-9710-6
[26] Mehdad, A.; Gould, N. S.; Xu, B.; Lobo, R. F. Effect of Steam and CO_2 on Ethane Activation over Zn-ZSM-5. *Catal. Sci. Technol*. **2018**, *8*, 358–366. https://doi.org/10.1039/C7CY01850A
[27] Patrylak, L.; Konovalov, S.; Yakovenko, A.; Pertko, O.; Povazhnyi, V.; Kurmach, M.; Voloshyna, Y.; Filonenko, M.; Zubenko, S. Fructose Transformation into 5-Hydroxymethylfurfural over Natural Transcarpathian Zeolites. *Chem. Chem. Technol*. **2022**, *16*, 521–531. https://doi.org/10.23939/chcht16.04.521
[28] Voloshyna, Y.; Pertko, O.; Povazhnyi, V.; Patrylak, L.; Yakovenko, A. Effect of Modifying the Clinoptilolite-Containing Rocks of Transcarpathia on Their Porous Characteristics and Catalytic Properties in the Conversion of C_6-Hydrocarbons. *Chem. Chem. Technol*. **2023**, *17*, 373–385. https://doi.org/10.23939/chcht17.02.373
[29] Saputra, E.; Budihardjo, M. A.; Bahri, S.; Pinem, J. A. Cobalt-Exchanged Natural Zeolite Catalysts for Catalytic Oxidation of Phenolic Contaminants in Aqueous Solutions. *J. Water Process Eng*. **2016**, *12*, 47–51. https://doi.org/10.1016/j.jwpe.2016.05.012
[30] Inchaurrondo, N. S.; Font, J. Clay, Zeolite and Oxide Minerals: Natural Catalytic Materials for the Ozonation of Organic Pollutants. *Molecules* **2022**, *27*, 2151. https://doi.org/10.3390/molecules27072151
[31] Abdulloh, A.; Rahmah, U.; Permana, A. J.; Mahdy, A. A.; Budiastanti, T. A.; Fahmi, M. Z. Cracking Optimization of Palmitic Acid Using Fe^{3+} Modified Natural Mordenite for Producing Aviation Fuel Compounds. *Chem. Chem. Technol*. **2023**, *17*, 625–635. https://doi.org/10.23939/chcht17.03.625
[32] Himpsl F.L. Method for Producing Cracking Catalyst. US4581341, April 8, 1986.
[33] Álvarez, A.; Borges, M.; Corral-Pérez, J. J.; Olcina, J. G.; Hu, L.; Cornu, D.; Huang, R.; Stoian, D.; Urakawa, A. CO_2 Activation over Catalytic Surfaces. *ChemPhysChem* **2017**, *18*, 3135–3141. https://doi.org/10.1002/cphc.201700782

Received: November 08, 2024 / Revised: April 10, 2025 / Accepted: June 03, 2025

ОКИСНЕ ДЕГІДРУВАННЯ н-БУТАНУ ЗА УЧАСТЮ CO_2 НА МІКРОСФЕРИЧНИХ ЦЕОЛІТОВМІСНИХ КОМПОЗИТАХ НА ОСНОВІ УКРАЇНСЬКОГО КАОЛІНУ

Анотація. *У цьому дослідженні на основі українського каоліну синтезовано цеолітовмісні мікросферичні композити і модифіковано їх сполуками амонію, лантану та цирконію. Модифіковані композити деалюміновано термопаровою обробкою. Одержані матеріали охарактеризовано з використанням низки фізико-хімічних методів і протестовано в реакції окисного дегідрування н-бутану за участю CO_2. Проаналізовано вплив ряду чинників на характеристики синтезованих зразків і пов'язані з цим зміни їхньої активності і селективності. Результати роботи показали принципову можливість використання таких композитів як каталізаторів цієї реакції.*

Ключові слова: *каолінова мікросфера, цеоліт FAU, композитний каталізатор, перехідний метал, окисне дегідрування, н-бутан.*